J Physiol 587.4 (2009) pp 753–768

The Journal of Physiology

GABAergic activities enhance macrophage inflammatory protein-1α release from microglia (brain macrophages) in postnatal mouse brain

Giselle Cheung[1], Oliver Kann[2], Shinichi Kohsaka[3], Katrin Fäerber[1] and Helmut Kettenmann[1]

[1] *Cellular Neurosciences, Max-Delbrueck-Center for Molecular Medicine, Robert-Roessle-Strasse 10, D-13092 Berlin, Germany*
[2] *Institute for Neurophysiology, Charité – Universitaetsmedizin Berlin, Tucholskystrasse 2, D-10117 Berlin, Germany*
[3] *Department of Neurochemistry, National Institute of Neuroscience, Kodaira, Tokyo 187-8502, Japan*

Microglial cells (brain macrophages) invade the brain during embryonic and early postnatal development, migrate preferentially along fibre tracts to their final position and transform from an amoeboid to a ramified morphology. Signals by which the invading microglia communicate with other brain cells are largely unknown. Here, we studied amoeboid microglia in postnatal corpus callosum obtained from 6- to 8-day-old mice. These cells accumulated on the surface of acute brain slices. Whole-cell patch-clamp recordings revealed that the specific $GABA_A$ receptor agonist muscimol triggered a transient increase in conductance typical for inward rectifying potassium channels in microglia. This current increase was not mediated by microglial $GABA_A$ receptors since microglial cells removed from the slice surface no longer reacted and cultured microglia only responded when a brain slice was placed in their close vicinity. Muscimol triggered a transient increase in extracellular potassium concentration ($[K^+]_o$) in brain slices and an experimental elevation of $[K^+]_o$ mimicked the muscimol response in microglial cells. Moreover, in adult brain slices, muscimol led only to a minute increase in $[K^+]_o$ and microglial cells failed to respond to muscimol. In turn, an increase in $[K^+]_o$ stimulated the release of chemokine macrophage inflammatory protein-1α (MIP1-α) from brain slices and from cultures of microglia but not astrocytes. Our observations indicate that invading microglia in early postnatal development sense GABAergic activities indirectly via sensing changes in $[K^+]_o$ which results in an increase in MIP1-α release.

(Resubmitted 24 September 2008; accepted after revision 27 November 2008; first published online 1 December 2008)
Corresponding author H. Kettenmann: Cellular Neurosciences, Max-Delbrueck-Center for Molecular Medicine, Robert-Roessle-Strasse 10, D-13092 Berlin, Germany. Email: kettenmann@mdc-berlin.de

Microglia are of mesodermal origin, share many features with monocytes and invade the central nervous system (CNS) early in development (Perry *et al.* 1985; Cuadros & Navascues, 2001). del Rio-Hortega (1932) found that the microglial progenitors, or microgliocytes as he called them, are characterized by amoeboid morphology and have preferred regions of invasion. One of those regions is the supraventricular corpus callosum. These immature microglial cells use axon tracts and vessels as guiding structures. As a consequence, migrating microglial cells accumulate in white matter tracts such as in the corpus callosum in early postnatal days. These highly motile microglial cells perform active phagocytosis of cellular debris in response to naturally occurring cell death (Ferrer *et al.* 1990; Brockhaus *et al.* 1996). Using postnatal acute brain slices, invading amoeboid microglia can be studied with imaging or patch-clamp techniques. They actively scan the slice surface with their processes and express prominent inward-rectifying K^+ channels (K_{ir}; Brockhaus *et al.* 1993) similar to microglia *in vitro* (Kettenmann *et al.* 1990). Recent evidence indicates that microglial properties like motility and migration, phagocytosis, release of cytokines and reactive oxygen species are modulated by neurotransmitters (Pocock & Kettenmann, 2007). For amoeboid microglia, functional expression of purinergic (Haas *et al.* 1996), adrenergic and dopaminergic (Färber *et al.* 2005) receptors have been described.

The majority of microglial studies have focused on their roles in pathology (Aloisi, 2001; Bajetto *et al.* 2002). It is well established that microglia, activated by a pathological event, recruit haemopoietic cells by the release of chemokines such as keratinocyte-derived chemokine (KC), macrophage inflammatory protein-1α/β

This paper has online supplemental material.

DOI: 10.1113/jphysiol.2008.163923

(MIP1-α/β), MIP2, monocyte chemoattractant protein-1 (MCP-1), RANTES, γ interferon, inducible protein-10 (IP-10) and IL-8 (Hanisch, 2002; Ambrosini & Aloisi, 2004). Recent studies have provided strong evidence that chemokines including stromal cell-derived factor-1 (SDF-1), RANTES, MCP-1, MIP1-α, IL-8, KC and fractalkine appear to regulate developmental processes (Ambrosini & Aloisi, 2004; Rostene *et al.* 2007). Since microglial cells are an important source of chemokines in the CNS, they have the potential to regulate brain development.

The formation of neuronal circuits during brain development requires intricate mechanisms involving different cell types and signalling molecules. γ-Amino-butyric acid (GABA) is released from growth cones of developing axons prior to synapse formation (Gao & van den Pol, 2000) and acts as a trophic factor in the developing brain. Microglial cells have been shown to express $GABA_B$ receptors (Kuhn *et al.* 2004), but at present there is no evidence for functional $GABA_A$ receptors in microglia. In the present study we have addressed the question of whether GABA will affect microglial properties in the developing brain.

Methods

Animals

Wild-type Naval Medical Research Institute (NMRI) mice were provided by Charles River Laboratories (Sulzfeld, Germany). Transgenic mice expressing enhanced green fluorescent protein (EGFP) under the control of the ionized calcium binding adaptor molecule 1 (Iba1) and glial fibrillary acidic protein (GFAP) promoters were previously described (Nolte *et al.* 2001; Hirasawa *et al.* 2005). All animals were bred and maintained in our institutional animal facility. All experimental procedures were approved by official committees and adhere to institutional guidelines.

Acute brain slice preparation

Acute brain slices were prepared from postnatal (postnatal days (P)6–8) and adult (P35–40) mice as previously described (Haas *et al.* 1996). In brief, mice were decapitated and brains were carefully removed and washed in standard brain slice buffer containing (in mM): NaCl 134; KCl 2.5; $MgCl_2$ 1.3; $CaCl_2$ 2; K_2HPO_4 1.25; $NaHCO_3$ 26; D-glucose 10; pH 7.4. The buffer solution was saturated with carbogen (95% O_2, 5% CO_2). Coronal slices of 150 μm were made at 4°C using a vibratome (Leica, Heidelberg, Germany). They were then gently transferred and maintained in brain slice buffer at room temperature (21–25°C) until used.

Cell cultures

Primary cultures of astrocytes and microglia were prepared from cerebral cortex of newborn NMRI mice as previously described (Prinz *et al.* 1999; Kresse *et al.* 2005). In brief, cortical tissue freed of blood vessels and meninges was trypsinized for 2 min. It was then dissociated with a fire-polished pipette and washed twice. Mixed glial cells were cultured in Dulbecco's modified Eagle's medium (DMEM) supplemented with 10% fetal calf serum (FCS), 2 mM L-glutamine, and antibiotics (100 units ml^{-1} penicillin and 100 $\mu g\ ml^{-1}$ streptomycin). After 9–12 days with a medium change every third day, microglial cells were separated from the underlying astrocytic layer by gentle shaking for 1 h at 37°C with a shaker incubator (100 r.p.m.). Cells were then seeded on glass coverslips or 96-well plates at a density of 5×10^4 per coverslip or 2×10^5 cells per well, respectively. Primary cultures of microglia and astrocytes typically contained $> 95\%$ microglial cells or $> 90\%$ astrocytes as detected by a microglia marker, *Griffonia simplicifolia* isolectin B4 (Sigma) or an antibody against GFAP (DAKO, Hamburg, Germany), respectively. Plated cells were used for experiments within 1–3 days after plating. Cell media and supplements were purchased from Seromed/Biochrom (Berlin, Germany). Microglial depletion was performed with clodronate liposomes prepared according to previously described protocols (Van Rooijen & Sanders, 1994).

Electrophysiological recordings

Acute brain slices or culture coverslips were placed in a holding chamber mounted on the stage of an upright light microscope (Axioskop, Zeiss, Jena, Germany). To maintain constant condition during experiments, the chamber was continuously perfused with standard brain slice or Hepes buffer for brain slices or cultures, respectively, at 4–6 ml min^{-1}. Hepes buffer contained (in mM): NaCl 150; KCl 5.4; $CaCl_2$ 2; $MgCl_2$ 1; Hepes 5; D-glucose 10 at pH 7.4. Amoeboid microglia accumulated on the surface of postnatal brain slices at the corpus callosum region which became evident 1 h after the slice preparation. They could be identified by their distinctive morphology under light microscopy as previously described (Brockhaus *et al.* 1993). Acute brain slices obtained from Iba1- and GFAP-EGFP mice were used to selectively observe microglia and astrocyte populations, respectively. EGFP-positive cells were identified using an excitation beam at 488 nm generated by a monochromator (Polychrome IV, Till Photonics, Martinsried, Germany). The emitted light was collected at 530 ± 10 nm. Patch pipettes were pulled from borosilicate capillaries (inner diameter 0.87 mm; outer diameter 1.5 mm; Hilgenberg, Malsfeld, Germany) using a P-2000 laser-based pipette

puller (Sutter Instrument Co., Novato, CA, USA) and filled with pipette solution containing (in mM): KCl 130; $MgCl_2$ 2; $CaCl_2$ 0.5; Hepes 10; EGTA 5 at pH 7.3. To confirm intracellular access, Alexa Fluor 594 (10 μg ml^{-1}, Invitrogen, Karlsruhe, Germany) was added to the pipette solution. Pipette resistance ranged from 5 to 8 MΩ. Whole-cell voltage-clamp experiments were performed according to previously described protocols (Hamill *et al.* 1981). Currents filtered at 2.9 kHz were recorded using an EPC-9 amplifier coupled to TIDA software (HEKA Electronics, Lambrecht, Germany). Capacitative transients and series resistance were compensated by the software. Membrane potential and resistance were measured on screen. Only cells with stable membrane potential throughout measurements were used. Drug application was achieved by changing the perfusate. The time of perfusion exchange was determined by measuring the time course of an increase in $[K^+]_o$ by K^+-sensitive microelectrodes in the chamber and within the slice. The time constant of exchange was 22 ± 4 s ($n = 15$) in the chamber and 80 ± 6 s ($n = 8$) in the slices. A sample trace is shown in Supplemental Fig. 1 of the online Supplemental material. All experiments were performed at room temperature.

Extracellular potassium measurement

Recordings of extracellular potassium concentration ($[K^+]_o$) in acute brain slices were performed according to previously described protocols (Heinemann & Arens, 1992; Kann *et al.* 2003). Changes in $[K^+]_o$ were recorded with double-barrel microelectrodes from theta glass (Science Products, Hofheim, Germany). One barrel was filled with 154 mM NaCl and served as a reference channel; the other barrel was filled with K^+ ionophore I cocktail A (60031; Fluka Chemie, Buchs, Switzerland) and 100 mM KCl, and served as the ion-sensitive channel. The amplifier was equipped with negative capacitance feedback control, which permitted recordings of changes in $[K^+]_o$ with time constants of 50–200 ms. Changes in voltage were digitized at 10 Hz using FeliX software (Photon Technology Instruments, Wedel, Germany). To translate the recorded potential values (mV) in $[K^+]_o$, a modified Nernst equation was used (Heinemann & Arens, 1992; Kann *et al.* 2003): $\log[\mathrm{Ion}]_1 = E_M(s \times v)^{-1} + \log[\mathrm{Ion}]_0$, where E_M represents recorded potential; s, electrode slope obtained at calibration; v, valency of the specific ion; $[\mathrm{Ion}]_0$, ion concentration at rest; and $[\mathrm{Ion}]_1$, ion concentration during activation.

Microchemotaxis assay

Microglial migration assay was performed in 48-well microchemotaxis chambers (Neuroprobe, Gaithersburg, MD, USA) as previously described (Nolte *et al.* 1996). Test substances diluted in serum-free DMEM were added to each of the lower wells. Upper and lower wells were separated by a polycarbonate filter with a pore size of 8 μm (Poretics Corp., Livermore, CA, USA). Cultured microglia were added to the upper wells (4×10^4 per well), and the chamber was incubated at 37°C and 5% CO_2 for 2 h. Filters were then removed and stained for microglia with Diff-Quik-Fix stain set (Medion Diagnostics, Düdingen, Switzerland) according to the manufacturer's instructions. The rate of microglial migration was calculated by counting cells in four random fields of each well and normalized to control conditions.

Microglial proliferation assay

Microglial cells plated in 96-well plates were treated for 24 or 48 h with the test substance in the presence of 10 μM bromodeoxyuridine (BrdU) diluted in DMEM/10% FCS. Proliferation was assessed using BrdU labelling and detection kit (Roche, Mannheim, Germany) according to the manufacturer's instructions. The amount of BrdU incorporated by cells after the treatment period was taken as a measure of proliferation. The resulting colorimetric reaction product was measured at 405 nm against 490 nm using a microplate reader (Perkin Wallac, Freiburg, Germany). Proliferation was normalized to control conditions.

Cytokine and chemokine quantification

To determine chemokine released *in situ*, 150 μm-thick half-hemispheres of postnatal corpus callosum slices were stored in 96-well plates in standard brain slice buffer while maintaining 5% CO_2 and 95% O_2 at pH 7.4. After at least 1 h of resting period, slices were washed once with buffer and incubated with test substances for 1.5 or 3 h. For cytokine and chemokine released *in vitro*, cells plated in 96-well plates were treated for 1.5, 3 or 24 h with test substances diluted in DMEM/10% FCS. Buffer or culture medium was collected after treatment periods and measured for the amount of IL-6, IL-12, KC, tumour necrosis factor-α (TNF-α), and MIP1-α using enzyme-linked immunosorbent assay (ELISA) according to the manufacturer's instructions (R&D Systems, Wiesbaden, Germany). The resulting colorimetric reaction product was measured at 450 nm against 540 nm using a microplate reader (Perkin Wallac). Cytokine and chemokine release was normalized to control conditions. Standard curves ranging from 125 to 4000 pg ml^{-1} were obtained using respective protein standards.

Cell viability test

Lactate dehydrogenase (LDH) cytotoxicity detection kit was used for quantification of cell viability according to the manufacturer's instructions (Roche, Mannheim, Germany). The colorimetric assay was quantified at 490 nm against 620 nm using a microplate reader (Perkin Wallac). The measurement of the activity of LDH released from the cytosol of damaged cells into the supernatant was taken as a measure of cell death and lysis in microglial cultures treated with the test substance.

Statistical analysis

Statistical analyses were performed using Microsoft Excel and Origin (OriginLab, Northampton, MA, USA) software. Differences between groups were evaluated by two-sample Student's *t* test. *P* values < 0.05 were considered statistically significant with $^{*}P < 0.05$; $^{**}P < 0.01$.

Results

Muscimol triggers an inward K^+ conductance in amoeboid microglia

To study electrophysiological properties of invading microglia in the developing mouse brain, we used acute brain slices obtained from P6–8 mice. Amoeboid microglia were recognized on the surface of corpus callosum acute slices by their distinct morphology (Fig. 1*A*) and their characteristic inwardly rectifying membrane current pattern as previously reported (Haas *et al.* 1996). The latter was recorded after clamping the membrane to a series of de- and hyperpolarizing voltage steps ranging from −170 to +50 mV from a holding potential of −70 mV (Fig. 1*B*). In addition, we also made slices from Iba1-EGFP transgenic animals in which microglia are labelled by EGFP (Supplemental Fig. 2*A*) or by incubation of the slices for 40 min with fluorescently (Alexa Fluor 594) labelled tomato lectin (60 μg ml^{-1}), a marker for microglial cells. To test for the effect of the

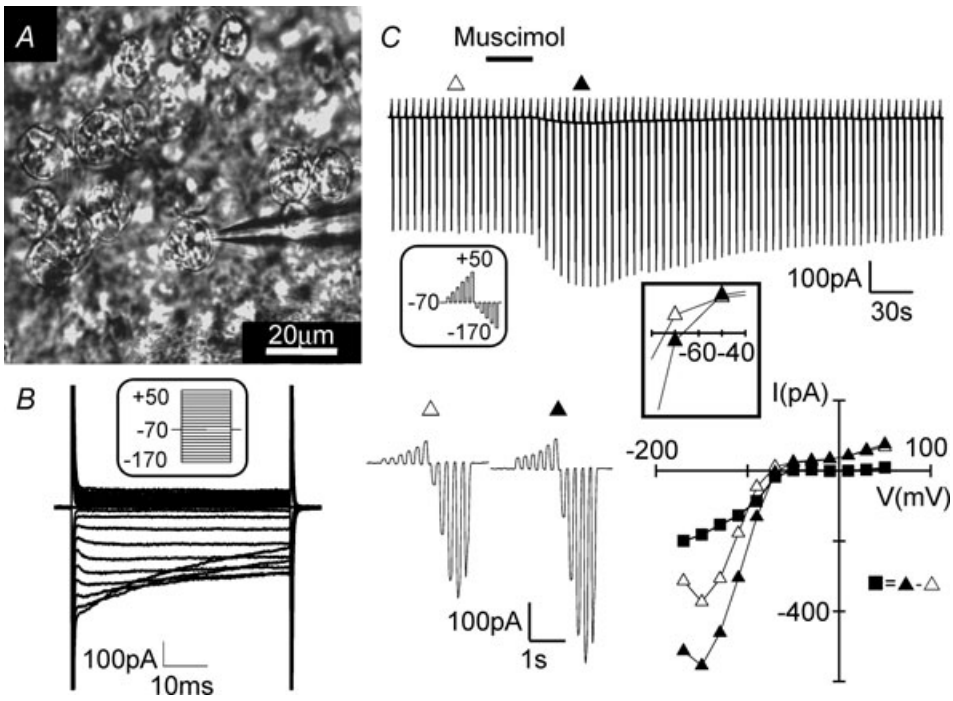

Figure 1. Muscimol-induced current response in amoeboid microglia
A, image of amoeboid microglia on the surface of a postnatal corpus callosum brain slice. One cell was approached with a patch pipette. *B*, membrane currents were recorded from de- and hyperpolarizing voltage steps ranging from −170 to +50 mV from a holding potential of −70 mV with 10 mV increments (see inset). *C*, membrane currents were recorded by voltage steps of the same range as in *B* but with 20 mV increments (see inset). Bath application of muscimol (100 μM; 30 s) induced current changes in this cell as shown. A series of voltage steps before (△) and during (▲) the muscimol-induced response are shown at a higher time resolution. The current–voltage plot was made from △, ▲ and ■ = ▲ − △ (muscimol-induced current). The inset shows the current–voltage relationship close to the membrane potential.

specific $GABA_A$ receptor agonist muscimol (100 μM), the series of voltage jumps was repetitively applied (every 5 s). When muscimol was applied via the bath solution for 30 s, the current elicited with hyperpolarizing voltage jumps increased (Fig. 1*C*). At −170 mV, the increase amounted to 130 ± 23 pA ($n = 32$; $P < 0.01$). The peak response was reached after 21 ± 2 s and returned to baseline after 149 ± 2 s. An increase at the peak response was considered significant when it was above a threshold of three times membrane noise standard deviation. Moreover, we found that muscimol elicited only one response in each cell. A second muscimol application even after a 10 min washout did not trigger a response ($n = 8$; Fig. 2*A*). The cells were, however, still responsive to 1 mM ATP. In the presence of the $GABA_A$ receptor antagonist gabazine (10 μM; 1.5 min pre-application), we only observed a response to muscimol in 20% of cells ($n = 10$; Fig. 2*B*). This response was significantly smaller compared to the muscimol response (47 ± 5 pA at −170 mV; $P < 0.01$) in the absence of the antagonist. Furthermore, we can show that muscimol-induced current response can be blocked by the K^+ channel blocker $BaCl_2$ (100 μM), in 8 out of 9 cells (Fig. 2*C*) and was unaffected by addition of 0.5 μM tetrodotoxin (TTX; $n = 5$; data not shown).

We also recorded from tomato lectin-positive microglial cells located within the slice tissue. These cells showed a similar response to bath application of muscimol as the amoeboid cells on the surface ($n = 6$; Supplemental Fig. 2*B*). In addition, we have also tested the effect GABA and observed a similar inward current response in amoeboid microglia. However, the amplitude was much smaller as compared to muscimol ($25 \pm 3\%$, $n = 5$; data not shown). The smaller response to GABA could be explained by GABA uptake and therefore, the specific $GABA_A$ agonist muscimol was used throughout this study.

The muscimol-induced current response is mediated by a factor released from the slice

To test whether muscimol directly stimulates microglial cells or indirectly by the release of a factor from the slice, we tested muscimol on amoeboid microglial cells after removal from the slice. After establishing the seal with the recording pipette using the whole-cell patch-clamp configuration, amoeboid microglia were carefully lifted up from the surface of the slice as illustrated in Fig. 3*A*. The cells were maintained for 5 min and then muscimol (100 μM) was applied for 30 s. Whereas 100% of cells showed a muscimol-induced response at the surface, 5 out of 6 and only 3 out of 15 cells responded at a distance of 150 and 300 μm, respectively (Fig. 3*B*). In cells which showed a muscimol-induced response at 150 and 300 μm, the inward current was 39 ± 13 pA and 20 ± 7 pA for the −170 mV voltage jump, respectively, thus 30% and 16% of the average response at the surface. As a control, the response to ATP (0.5–1 mM) following muscimol application did not significantly change in relation to the distance from the slice.

To establish that muscimol triggers the release of a factor from brain slices that induces a response in microglia, we tested for the responsiveness of microglial cells from primary cultures towards muscimol. We also placed a brain slice of a half-hemisphere on the coverslip with the microglial culture (Fig. 3*C*). After observing that muscimol (100 μM) did not trigger a current response in microglial cells in culture ($n = 43$, Fig. 3*D* left trace), we recorded the membrane current response to muscimol

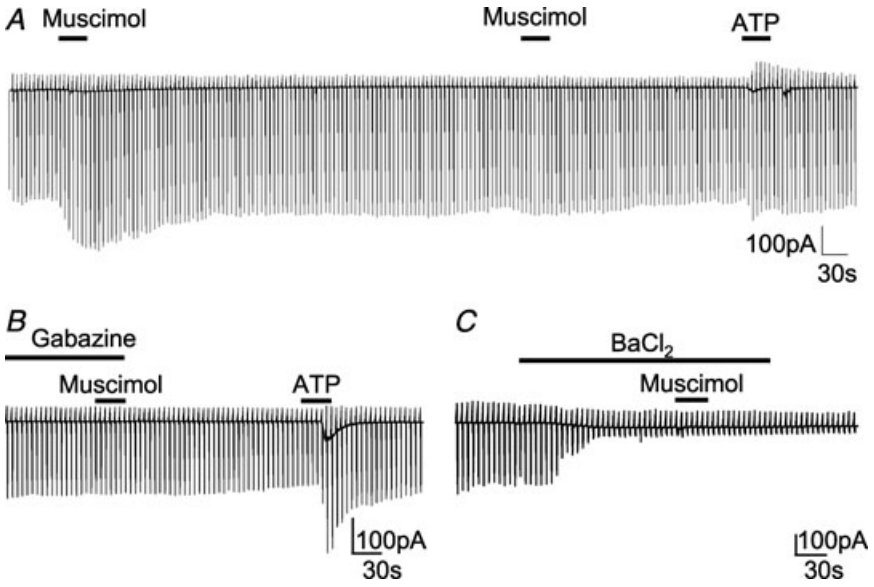

Figure 2. $GABA_A$ receptor-specific muscimol-induced current response in amoeboid microglia
Membrane currents from amoeboid microglia were recorded in response to voltage steps as described in Fig. 1*C*. The individual voltage steps cannot be resolved at this low time resolution display. *A*, muscimol (100 μM; 30 s) was applied twice interrupted by a 10 min interval. After another 3 min, ATP was applied (500 μM; 30 s). *B*, muscimol (100 μM; 30 s) was also applied in the presence of gabazine (10 μM; 1.5 min pre-application) followed by ATP (1 mM; 30 s). *C*, muscimol (100 μM; 30 s) was applied in the presence of $BaCl_2$ (100 μM; 2 min pre-application).

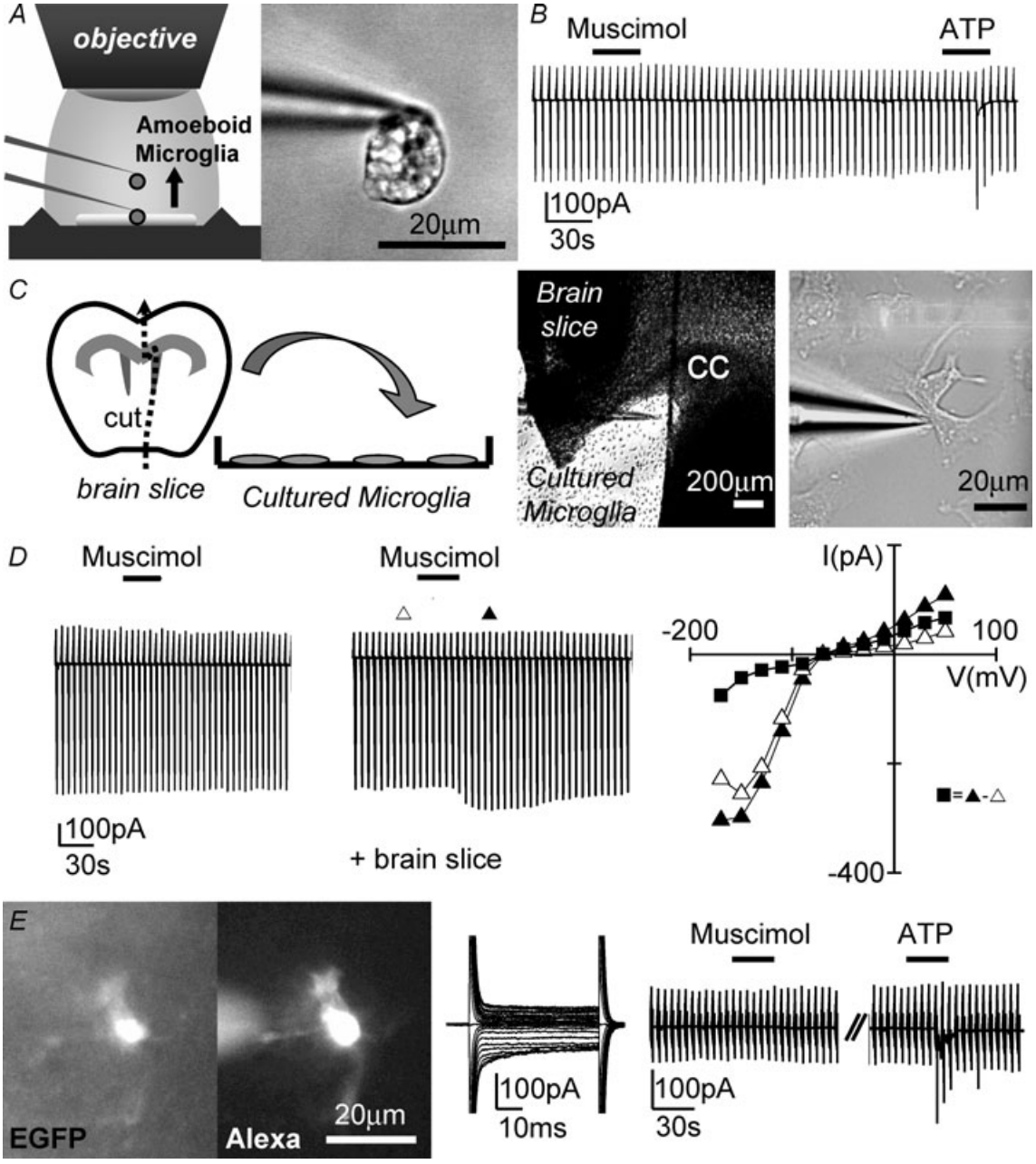

Figure 3. Muscimol-induced current responses in microglia are only observed in the vicinity of postnatal brain slice

A, illustration showing how an amoeboid microglial cell could be lifted up from the brain slice while still attached to the patch pipette (left). Image of a cell lifted up 300 μm from the slice (right). *B*, membrane currents were recorded as described in Fig. 1*C* while muscimol (100 μM; 30 s) was applied. ATP (500 μM; 30 s) was applied as a positive control 4 min later. *C*, an illustration showing how the brain slice was cut into half-hemispheres and one was placed on a coverslip with cultured microglial cells (left). Images showing the brain slice and a cultured microglial cell approached with the patch pipette at high and low resolutions (right). *D*, similar to *B*, membrane currents of cultured microglial cells were recorded during muscimol (100 μM; 30 s) application in the absence (left) and presence of a brain slice (middle). The current–voltage plot was made from △, ▲ and ■ = ▲ – △ (muscimol-induced current). *E*, a ramified microglial cell in the cortex close to the corpus callosum in an acute brain slice prepared from an adult (P35–40) Iba1-EGFP transgenic mouse is shown. EGFP fluorescence and the same cell filled with Alexa Fluor 594 (10 μg ml^{-1}) via the patch pipette are shown (left). Membrane currents typical for a ramified microglial cell were recorded as described in Fig. 1*B* (middle). Similar to *B*, membrane currents were recorded while applying muscimol (100 μM; 30 s) and ATP (1 mM; 30 s) 5 min apart.

from a cultured microglial cell close to the brain slice. Eighty-nine per cent of primary cultured microglial cells in close vicinity to the slice (within 1 mm distance) responded with an increase in inward current in response to muscimol similar to that observed in amoeboid microglia on brain slices ($n = 18$; Fig. 3*D* middle trace and right-hand current–voltage plot). The muscimol-triggered current recorded at -170 mV (-43 ± 6 pA) was, however, significantly smaller ($P < 0.05$) than that observed in amoeboid microglia from brain slices. The peak of the muscimol-induced response was reached 22 ± 3 s after muscimol application. These results demonstrate that $GABA_A$ receptor activation in acute brain slices from early postnatal age induced the release of an intrinsic factor which stimulates microglial cells.

To analyse whether this $GABA_A$-mediated effect is specific for early postnatal development, we recorded membrane currents from microglial cells in acute brain slices obtained from adult (P35–40) Iba1-EGFP mice. The microglial cells had a ramified morphology as revealed by dye filling with Alexa Fluor 594 (10 μg ml^{-1}) included in the pipette. These cells were also characterized by small inward currents induced by hyperpolarizing voltage steps as previously described (Boucsein *et al.* 2000). Muscimol (100 μM) did not trigger any current response in any cell tested ($n = 8$; Fig. 3*E*).

An increase in $[K^+]_o$ mimics the muscimol-induced current in microglia

The conductance of inward rectifying channels increases with elevation in $[K^+]_o$ which has also been shown for microglial cells (Kettenmann *et al.* 1990). However, the impact of moderate changes in $[K^+]_o$ have not been tested. To test whether an increase in $[K^+]_o$ will mimic the effect of muscimol, we increased $[K^+]_o$ from the basal level of 5 mM to 7.5, 10 and 12.5 mM adding 2.5, 5 and 7.5 mM KCl, respectively, and measured membrane currents at a series of de- and hyperpolarized voltages as described above. As shown in Fig. 4*A* and *D*, the increase in $[K^+]_o$ dose-dependently increased the cord conductance of the inward rectifying current determined between -110 and -130 mV. The conductance increased significantly by 0.43 ± 0.25, 0.76 ± 0.17 and 1.25 ± 0.01 nS for the 2.5, 5 and 7.5 mM $[K^+]_o$ increase, respectively. Thus, the average muscimol-induced conductance increase of

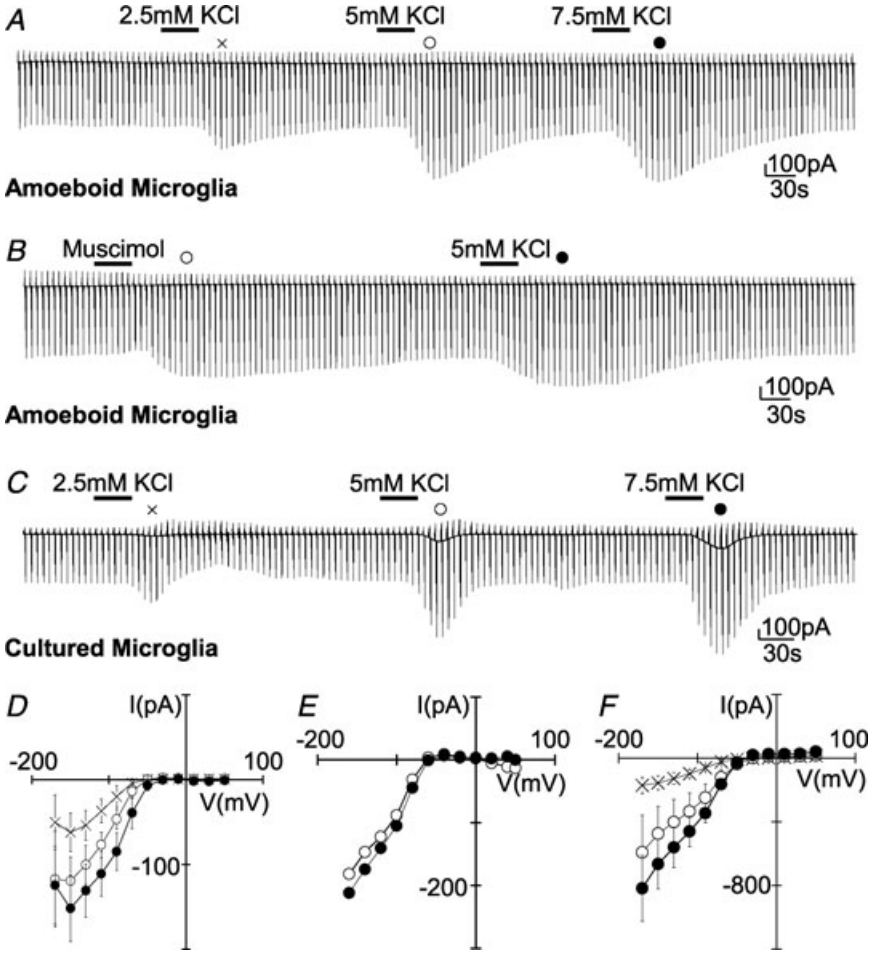

Figure 4. Increased $[K^+]_o$ mimics the muscimol-induced current response in microglia
Membrane currents were recorded as described in Fig. 1*C*. Current traces are shown for an amoeboid microglial cell while applying KCl (2.5, 5 and 7.5 mM; each for 30 s; *A*) and muscimol (100 μM; 30 s; *B*) followed by KCl (5 mM; 30 s; *B*). *C*, current traces obtained from a similar approach to that in *A* for a cultured microglial cell are shown. Note that the delayed decrease of inward current upon 2.5 mM KCl application is not typically observed. The addition of 2.5, 5 and 7.5 mM KCl increased $[K^+]_o$ from 5 to 7.5, 10 and 12.5 mM, respectively (*D–F*). Current–voltage plots were obtained by subtracting currents at the peak of the response from that prior to drug application as indicated above the current traces of *A*, *B* and *C*, respectively. *D* and *F* show mean ± S.E.M. values from 4 independent experiments.

0.81 ± 0.09 nS was similar to the increase triggered by 5 mM K^+ (Fig. 4*B* and *E*). A similar conductance increase by elevated $[K^+]_o$ was also obtained in cultured microglial cells. The conductance increased significantly by 1.74 ± 0.66, 3.32 ± 1.31 and 4.99 ± 1.61 nS for an elevation to 7.5, 10 and 12.5 mM (Fig. 4*C* and *F*). Thus, an increase in $[K^+]_o$ could explain the muscimol-induced conductance change both in the amoeboid microglia from the slice and the cultured microglial cells placed close to a slice.

Muscimol triggers an increase in $[K^+]_o$ within and on the surface of the brain slice

To test whether muscimol would induce an increase in $[K^+]_o$, we measured $[K^+]_o$ using K^+-sensitive microelectrodes. The electrodes were either placed on the surface of the slice close to the amoeboid microglia or inserted about 30 μm within the slice. When placed on the surface of the slice, a first application of muscimol (100 μM) for 30 s increased $[K^+]_o$ transiently from 5 to 7.5 ± 0.2 mM ($n = 6$; Fig. 5*A* and *E*). The peak of the increase was reached within 54 ± 7 s. The $[K^+]_o$ returned to baseline after 342 ± 18 s. A second or third application separated by 15 min washout induced a significantly smaller increase to only 5.7 mM ($n = 6$). In the presence of the $GABA_A$ receptor antagonist gabazine (with 2 min pre-application, 10 μM), muscimol failed to trigger an increase in $[K^+]_o$ ($n = 4$; Fig. 5*B* and *E*). With the K^+-sensitive microelectrodes inserted about 30 μm into the corpus callosum slice, a $[K^+]_o$ increase to 9.6 ± 0.8 mM was detected upon first application of 100 μM muscimol ($n = 4$; Fig. 5*C* and *E*), significantly greater than that observed at the surface. Subsequent responses were also smaller in amplitude as observed on the surface. We also analysed for potential differences in $[K^+]_o$ elevation between postnatal corpus callosum and cortical regions ($n = 6$; data not shown), but did not find any significant difference, either on the surface or within the slice, indicating that K^+ released to the extracellular space was similar in neighbouring brain regions. To study age-dependent K^+ release upon $GABA_A$ receptor stimulation, $[K^+]_o$ was measured in adult brain slices obtained from 35- to 40-day-old mice. Significantly smaller $[K^+]_o$ increases were observed both on the surface (to 5.6 ± 0.1 mM; $n = 5$) and within adult slices (to 6.5 ± 0.2 mM; $n = 3$) as compared to postnatal ones (Fig. 5*D* and *E*).

Macroglial cells in the corpus callosum show $GABA_A$ receptor-mediated responses

To study GABA responses in macroglial cells of the corpus callosum, astrocytes and oligodendrocytes, we identified cells by recording membrane currents at potentials ranging from −170 to +50 mV. Based on the current pattern, we could distinguish between three cell

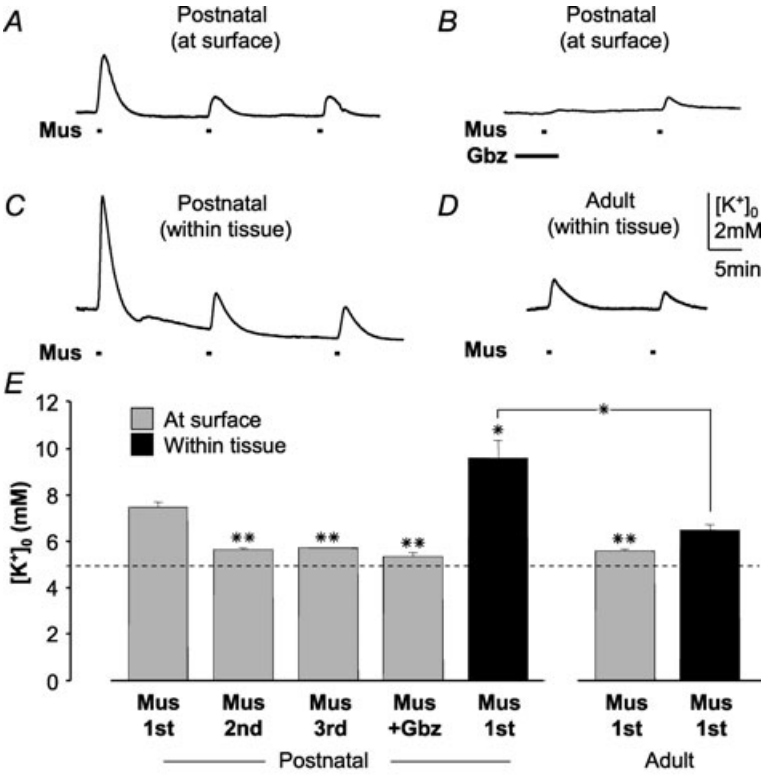

Figure 5. $[K^+]_o$ in brain slices during $GABA_A$ receptor stimulation
A K^+-sensitive microelectrode was used to measure $[K^+]_o$ during repetitive muscimol applications (Mus; 100 μM; 30 s; *A*) and muscimol application (Mus; 100 μM; 30 s; *B*) in the presence and absence of gabazine (Gbz; 10 μM; 2 min pre-application) at the surface of a postnatal (P6–8) corpus callosum slice. *C*, similar recording to that in *A*, but with the microelectrode placed 30 μm below the surface of the corpus callosum. *D*, similar recording to that in *C*, but from an adult (P35–40) corpus callosum slice. *E*, mean ± S.E.M. values of peak amplitudes are plotted from 6 independent experiments. First, second and third muscimol response and that in the presence of gabazine (Mus + Gbz) are shown. In all experiments, baseline $[K^+]_o$ was adjusted to 5 mM. $^*P < 0.05$, $^{**}P < 0.01$ compared to the first muscimol response unless indicated otherwise.

populations. As previously described, oligodendrocytes are characterized by a linear current–voltage curve with decaying currents and large tail currents (Berger *et al.* 1992). After injection with Alexa Fluor 594, we could recognize the processes orientated in parallel to the fibres, the typical morphological feature of oligodendrocytes (Fig. 6*A*). Similar to recordings for hippocampus, cortex or cerebellum, astrocytes (Fig. 7*A*) are characterized by a linear current–voltage curve without current decay (Müller *et al.* 1992; Steinhäuser *et al.* 1992; Schipke *et al.* 2001). In addition, we found a third population of cells with an outwardly rectifying current pattern (Fig. 6*B*) previously described as glial progenitor cells in the corpus callosum (Berger *et al.* 1991), complex cells or NG2 cells in the hippocampus and other brain regions (Bergles *et al.* 2000; Lin & Bergles, 2002; Lin *et al.* 2005; Ziskin *et al.* 2007). The astrocytes had processes with a diffuse appearance, while the glial progenitor cells were characterized by thin and elongated processes. In addition, we studied cells in slices from GFAP-EGFP transgenic mice in which astrocytes are strongly labelled by EGFP and could thus be distinguished from oligodendrocytes and glial progenitor cells. All three cell types responded to application of muscimol (100 μM; 30 s) with an inward current recorded at −70 mV. Oligodendrocytes responded to muscimol with an inward current of 171 ± 38 pA ($n = 4$; Fig. 6*A*) and glial progenitor cells with an inward current of 228 ± 52 pA ($n = 9$; Fig. 6*B*) and astrocytes with an inward current of 188 ± 39 pA ($n = 9$; Fig. 7*A*). To measure membrane conductance, we repetitively clamped the membrane to a series of potentials ranging from −170 to +50 mV with 20 mV increments. We generally observed that the resting conductance permanently decreased after application of muscimol, similar to previous reports for Bergmann glial cells (Müller *et al.* 1994) or astrocytes, oligodendrocytes and glial progenitor cells in the spinal cord (Pastor *et al.* 1995). In all the three cell types we observed a conductance increase when comparing current–voltage curves at the peak of the response and after washout. The current reversed at positive potentials ranging from 10 to 40 mV. It was, however, evident that the muscimol-induced current showed inward rectification. The extrapolated reversal potential of the current recorded at negative membrane potentials was closer to 0 mV.

We also recorded from neurons which were located in the cortex at the border of the corpus callosum. These cells were identified by their large Na^+ currents and their ability to generate action potentials (data not shown). The muscimol-triggered inward current at −70 mV was 1129 ± 130 pA ($n = 13$), thus significantly

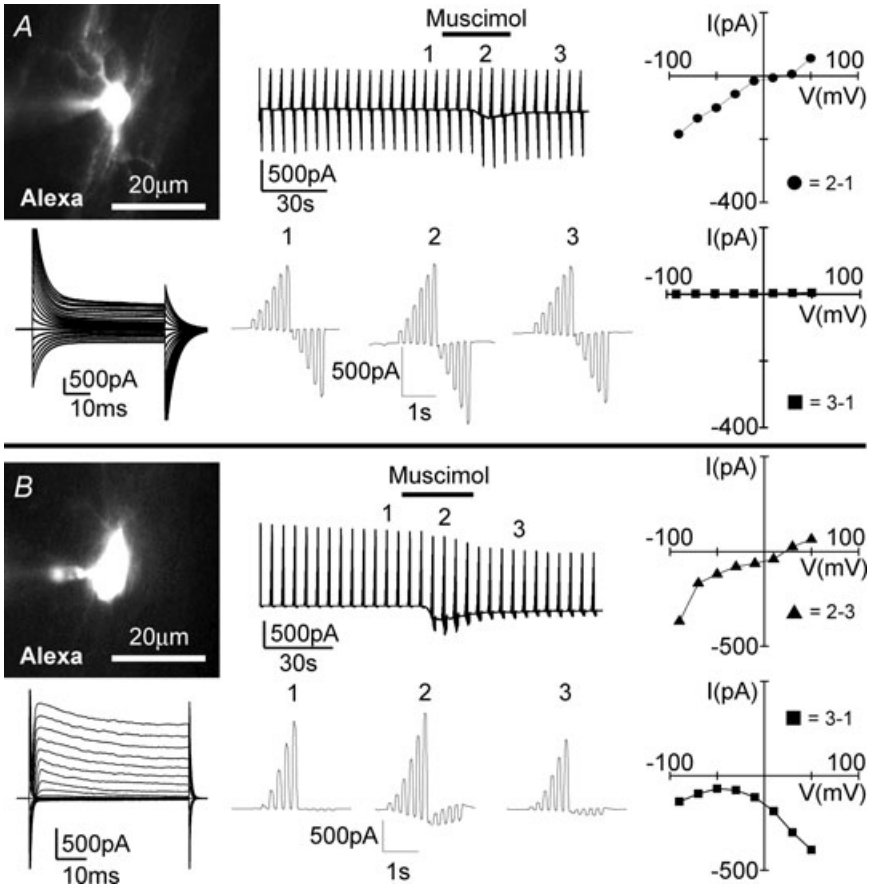

Figure 6. Muscimol-induced current response from an oligodendrocyte and a glial progenitor cell in the corpus callosum
An oligodendrocyte with characteristic tail current (*A*) and a glial progenitor cell with voltage-gated membrane current (*B*) in the neighbourhood of amoeboid microglia in the postnatal corpus callosum were voltage-clamped. Images of cells filled with Alexa Fluor 594 (10 μg ml^{-1}) via patch pipette are shown (top left). Membrane currents (top middle and bottom left) were recorded as described in Fig. 1 in response to muscimol (100 μM; 30 s). Voltage steps before (1), during (2) and after (3) muscimol-induced response are shown at a higher time resolution (bottom middle). Current–voltage plots were obtained by subtracting current responses at various time points as indicated (right).

larger as in glial cells (Fig. 7*B*). Similar to glial cells and as previously reported for granule neurons of the cerebellum (Labrakakis *et al.* 1997), we observed a permanent decrease of the resting conductance after application of muscimol. The reversal potential at the peak of the response was at about 20 mV and, similar to glial cells, the extrapolated reversal potential from currents recorded at negative membrane potentials was close to 0 mV.

When muscimol was applied a second time after 15 min washout, a markedly smaller response was observed in complex cells ($n = 4$), neurons ($n = 3$) and oligodendrocytes ($n = 3$). To exclude a contribution of indirect effect via activation of glutamate receptors or action potentials, we studied muscimol-induced currents in the presence of α-amino-3-hydroxy-5-methyl-4-isoxazolepropionic acid (AMPA)/kainate receptor antagonist 2,3-dihydroxy-6-nitro-7-sulfamoyl-benzo[f]quinoxaline-2,3-dione (NBQX; 10 μM), *N*-methyl-D-aspartic acid (NMDA) receptor antagonist amino-5-phosphonovaleric acid (APV; 50 μM) and TTX (0.5 μM) in glial progenitor cells ($n = 3$) and oligodendrocytes ($n = 3$). We observed similar responses to those in control experiments (see Supplemental Fig. 3 for a sample trace). We conclude that macroglial cells in the corpus callosum express functional $GABA_A$ receptors.

Muscimol and increased $[K^+]_o$ potentiated basal MIP1-α release

MIP1-α release from corpus callosum brain slices into standard brain slice buffer was quantified by ELISA. After 1.5 h, muscimol (100 μM) and KCl (addition of 5 mM) led to a small, but significant increase in MIP1-α production to $117 \pm 5\%$ ($n = 15$) and $115 \pm 6\%$ ($n = 16$) of control, respectively (Fig. 8*A*). The effect of muscimol and KCl was not observed in the presence of $BaCl_2$ (100 μM). Similarly, the muscimol-induced MIP1-α production was blocked by gabazine (10 μM). The KCl effect was not mimicked by equimolar NaCl indicating that increased osmolarity did not play a role in the induced release. Addition of 10 mM KCl resulted in an even higher increase in MIP1-α production after 1.5 h ($130 \pm 7\%$ of control; $n = 11$). The relative increase in MIP1-α release induced by addition of 10 mM KCl was similar after 3 h, namely $127 \pm 9\%$ ($n = 13$). Shorter stimulation on longer-termed MIP1-α production was also tested. Brain slices were treated with

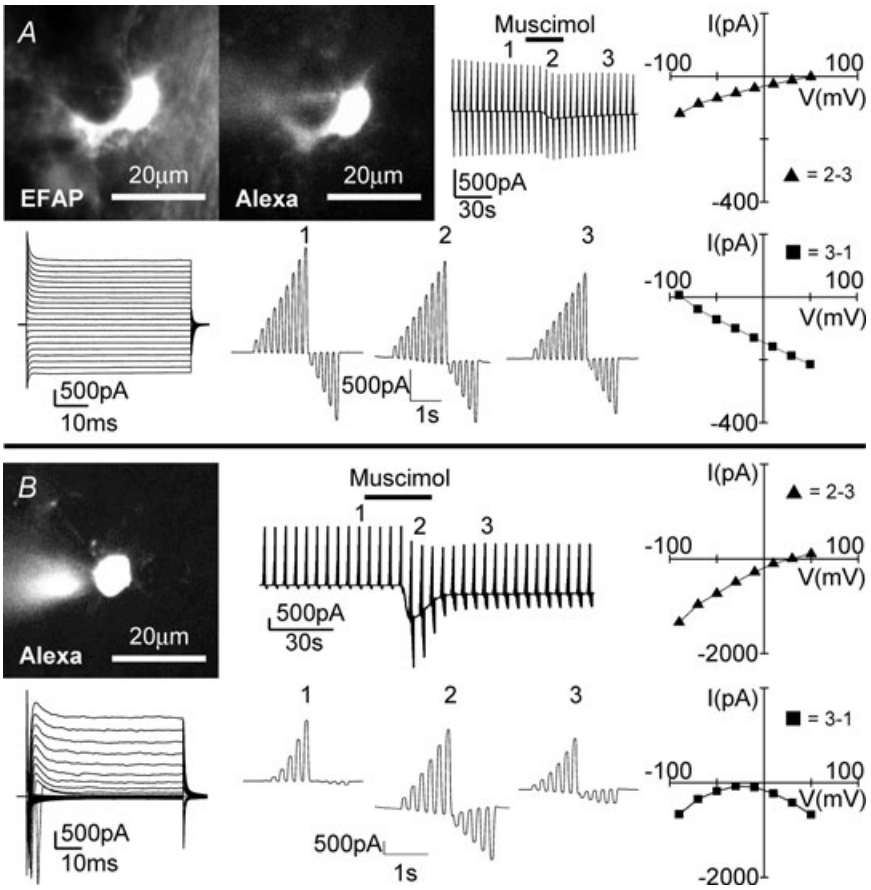

Figure 7. Muscimol-induced current response from an astrocyte in the corpus callosum and a neuron at the border of cortex to corpus callosum
A, an astrocyte with passive membrane current was identified by its strong EGFP fluorescence (top left) in a GFAP-EGFP transgenic animal. *B*, a cortical neuron close to the corpus callosum was also identified by large Na^+ currents in NMRI mice. Images of cells filled with Alexa Fluor 594 (10 μg ml^{-1}) via patch pipette are shown (top left). Membrane currents (top middle and bottom left) were recorded as described in Fig. 1 in response to muscimol (100 μM; 30 s). Voltage steps before (1), during (2) and after (3) muscimol-induced response are shown at a higher time resolution (bottom middle). Current–voltage plots were obtained by subtracting current responses at various time points as indicated (right).

muscimol or addition of 10 mM KCl for only 15 min. Total MIP1-α released after 1.5 h ($n = 8$) was not different from control indicating that prolonged stimulation was required (data not shown). It is feasible that a short application would lead to significant release but this cannot be measured in the supernatant.

To establish that the elevation in K^+ stimulates the MIP1-α release by microglial cells, we tested the effect of an increase in K^+ on microglial cultures. Cells plated on 96-well plates were treated with muscimol (100 μM) or addition of K^+ (5 and 10 mM) for 1.5, 3 and 24 h. Culture medium was collected and MIP1-α levels were determined by ELISA. Whereas muscimol had no effect, KCl dose-dependently enhanced microglial release of MIP1-α. In particular, 5 mM KCl induced an increase to $145 \pm 10\%$ of control after 24 h (4 independent experiments; Fig. 8*B*). KCl (20 mM), even enhanced MIP1-α release to $197 \pm 19\%$ of control at this time point (data not shown). Basal release of other cytokines, namely IL-6, IL-12, KC and TNF-α was not affected by either muscimol or KCl (data not shown). To assess MIP1-α release from astrocytes, primary astrocyte culture was used. Cells plated on 96-well plates were depleted of any residual microglia by treatment with clodronate liposomes for 24 h. We have demonstrated previously that clodronate selectively depleted microglial cells without affecting astrocytes and neurons in organotypic slice cultures (Markovic *et al.* 2005). Here, we observed that microglial depletion in astrocyte cultures significantly decreased the constitutive MIP1-α release to $76 \pm 2\%$ (data not shown). After microglia depletion, muscimol (100 μM) and KCl (addition of 5 and 10 mM) incubation for 1.5 and 3 h did not affect MIP1-α release into culture medium (4 independent experiments; Fig. 8*B*). As the effect of elevated K^+ on MIP1-α was observed in microglia but not astrocytes culture, we postulate that microglia are the source of K^+-induced MIP1-α release *in situ*.

As a control for cytotoxicity, we observed that 3 h incubation of microglial cultures with KCl (5 and 10 mM) and muscimol (100 μM) did not enhance LDH activity (3 independent experiments; data not shown).

Increased $[K^+]_o$ did not affect microglial chemotaxis nor proliferation *in vitro*

The ability of cultured microglia to migrate towards ATP in the presence of different concentrations of K^+ was assessed using a microchemotaxis chamber. Over the course of 2 h, 300 μM ATP alone significantly increased microglial migration rate to $226 \pm 27\%$ as compared to

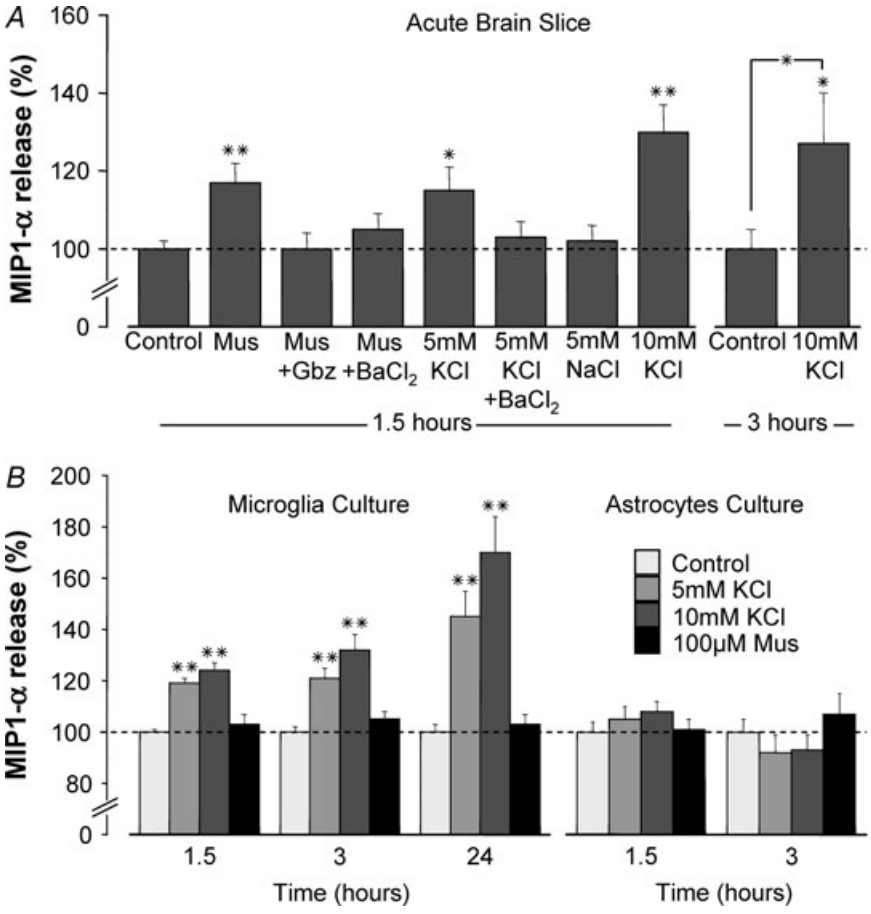

Figure 8. Effect of muscimol and $[K^+]_o$ elevation on MIP1-α release *in situ* and *in vitro*
Postnatal acute brain slices containing corpus callosum (*A*), and cultured microglia or astrocytes (*B*), were incubated with various substances for 1.5, 3 or 24 h. The amount of MIP1-α released into the standard brain slice buffer or culture medium was quantified by ELISA and normalized to corresponding controls at the same time point. KCl, 5 or 10 mM, was added resulting in a total $[K^+]_o$ of 10 or 15 mM; Mus = muscimol (100 μM); Gbz = gabazine (10 μM); $BaCl_2 = 100$ μM. NaCl (5 mM) was used as control for effect of osmotic changes. Results are expressed as mean ± S.E.M. values. $^*P < 0.05$; $^{**}P < 0.01$ compared with corresponding controls unless indicated otherwise.

control. However, no effect of increased $[K^+]_o$ on basal nor ATP-stimulated microglial migration was observed (5 independent experiments; data not shown). $[K^+]_o$ was elevated from 5 mM to 7.5, 10, 15, or 25 mM by addition of 2.5, 5, 10, or 20 mM KCl, respectively.

To assess the effect of increased $[K^+]_o$ on basal and lipopolysaccharide (LPS)-attenuated microglial proliferation, cultured microglia in 96-well plates were treated with different concentrations of KCl with or without LPS ($100\,ng\,ml^{-1}$) for 24 and 48 h in the presence of 10 μM BrdU. Proliferation was measured by the amount of BrdU incorporation relative to DMEM control. Whereas LPS significantly decreased control proliferation by 81 ± 7 and $54 \pm 7\%$ after 24 and 48 h, respectively, increase of $[K^+]_o$ by 2.5, 5, 10, or 20 mM did not affect basal or LPS-attenuated proliferation in microglia (6 independent experiments; data not shown).

Discussion

Here, we demonstrate that invading microglial cells could sense the activities of $GABA_A$ receptors in postnatal white matter. They responded to a GABA-mediated increase in $[K^+]_o$ by opening intrinsic K_{ir} channels. As a result, an enhanced release of MIP1-α was observed.

Macroglia in the corpus callosum and neurons in adjacent brain regions express functional $GABA_A$ receptors and are the presumed source for the GABA-mediated $[K^+]_o$ increase

Prior to synapse formation, when neuronal precursor cells and immature neurons begin to express functional $GABA_A$ receptors (Owens & Kriegstein, 2002), GABA is released from growth cones of developing axons (Gao & van den Pol, 2000). It occurs spontaneously and is enhanced by increased neuronal activity. At this stage of development, it acts as a trophic factor which modulates developmental processes like neuronal growth, migration, proliferation and differentiation and participates in the formation of synapse and construction of brain network (Ben-Ari *et al.* 2007). Thus, it is conceivable that GABA is released in the postnatal corpus callosum. Using a receptor-specific agonist muscimol, we observed that astrocytes, oligodendrocytes and glial precursor cells in the corpus callosum of postnatal brain slices as well as cortical neurons near this region express functional $GABA_A$ receptors. These observations are in line with our previous studies. A specific $GABA_A$ receptor-mediated current response was detected in cultured astrocytes (Bormann & Kettenmann, 1988) and oligodendrocytes (Von Blankenfeld *et al.* 1991). Berger *et al.* (1992) characterized $GABA_A$ receptors in glial precursors and pro-myelinating oligodendrocytes in mouse corpus callosum brain slices during the first 2 postnatal weeks. Astrocytic $GABA_A$ receptors were also well documented in the grey matter (Steinhäuser *et al.* 1994). In addition, complex glial cells in rat hippocampus responded towards $GABA_A$ but not $GABA_B$ receptor agonists (Bekar *et al.* 1999). Apart from muscimol-induced inward currents, we have also observed a sustained effect on K^+ currents which was previously described in glial cells and neurons (Müller *et al.* 1994; Pastor *et al.* 1995; Labrakakis *et al.* 1997). The activation of these two types of responses induced by muscimol, activation of a (presumably Cl^-) conductance and blockade of resting K^+ conductance resulted in a complex response with a reversal potential at positive voltages. In complex cells, there was no K^+ conductance at potentials negative to -70 mV and the extrapolated reversal potential was close to 0 mV. Furthermore, the muscimol-induced response was strongly reduced when elicited a second time even after a long washout period and receptor desensitization seemed likely. However, other possibilities such as receptor internalization or other mechanisms which can lead to a disappearance of the response could not be ruled out. Functions of glial $GABA_A$ receptors have been proposed as a way to sense neuronal activities (von Blankenfeld & Kettenmann, 1991), regulate extracellular pH (Kaila *et al.* 1991) and K^+ homeostasis (Barres *et al.* 1990). Although a recent study by Káradóttir *et al.* (2008) identified and characterized NG2 cells with large Na^+ currents and repetitive action potentials in the white matter of the cerebellum, we have not observed such cells in the corpus callosum.

GABA has a depolarizing action in the developing brain due to high $[Cl^-]_i$ (Ben-Ari *et al.* 2007). An increase in $[K^+]_o$ upon $GABA_A$ receptor stimulation is often observed as a result of membrane depolarization in immature neurons and glia leading to an efflux of K^+ and Cl^- (Hoppe & Kettenmann, 1989). GABA-mediated depolarization of glial precursor cells even activates Ca^{2+} channels (Kirchhoff & Kettenmann, 1992). Thus, it is likely that elevation of $[K^+]_o$ detected in postnatal brain slices is due to K^+ efflux from glial cells and/or immature neurons.

Muscimol-induced $[K^+]_o$ elevation was age dependent in that it was significantly smaller in adult brain slices. As neurons mature, $GABA_A$ receptors become inhibitory resulting in membrane hyperpolarization. This excitatory-to-inhibitory switch of GABA action in neurons begins during P5–8 (Leinekugel *et al.* 1995; Kuner & Augustine, 2000; Marandi *et al.* 2002).

Elevated $[K^+]_o$ increases conductance of intrinsic microglial K_{ir} channels

Our data indicate that microglial cells respond to GABA, not directly, but indirectly to a factor released in and from

the brain slice. This factor is K^+ and microglia respond to an increase in $[K^+]_o$ by an increase of their intrinsic K^+ current conductance. Amoeboid microglia at the corpus callosum of postnatal brain slices have similar membrane properties to those observed in cultured microglia despite their different morphology. Both amoeboid microglia and cultured microglia express prominent inwardly but no outwardly rectifying K^+ channels as previously described (Kettenmann *et al.* 1990; Brockhaus *et al.* 1993). The K_{ir} currents displayed time-dependent inactivation and can be blocked by extracellular Ba^{2+} at a range of 1–100 μM (Franchini *et al.* 2004). Muscimol and an increase in $[K^+]_o$ triggered an increase in membrane conductance which showed inward rectification and was sensitive to 100 μM $BaCl_2$, suggesting that it was mediated by intrinsic K_{ir} channels. K_{ir} channel activity is strongly dependent on $[K^+]_o$. An increase in $[K^+]_o$ from 4.5 to 50 mM increased the conductance of the channel more than twofold (Kettenmann *et al.* 1990). In the present study, moderate elevation in $[K^+]_o$ by 2.5, 5 and 7.5 mM from a baseline of 5 mM dose-dependently increased the inward K^+ conductance in amoeboid and cultured microglia. These experimental elevations in $[K^+]_o$ were clearly in the range of values obtained in brain slices because muscimol application mimicked the increase in $[K^+]_o$ by 5 mM. We thus conclude that muscimol does not directly activate $GABA_A$ receptors in microglial cells, but triggers a K^+ release from other cells and the resulting elevation in $[K^+]_o$ increases the conductance of the intrinsic inward rectifying channels. The increase of the conductance is due to the fact that permeability of inward rectifiers is strongly enhanced by an increase in $[K^+]_o$. As shown by Sakmann and Trube, the single channel conductance depends on the square root of $[K^+]$ (Sakmann & Trube, 1984). This is a general property of inward rectifiers but we have also shown this for microglial cells (Kettenmann *et al.* 1990). Moreover, at higher $[K^+]_o$ the channel loses its rectifying properties which explains the appearance of the outward current. Our experiments in acute slices were carried out at room temperature based on previous observations that responses are usually larger at lower temperatures (Kettenmann *et al.* 1987).

Basal MIP1-α release *in situ* and by cultured microglia is enhanced by elevated $[K^+]_o$ implying a potential role in postnatal development

Among various cytokines tested in this study, only MIP1-α release was affected by elevated $[K^+]_o$. Although constitutively expressed in low amounts, astrocytes and fetal microglia promptly synthesize and release MIP1 proteins *in vitro* upon stimulation (McManus *et al.* 1998; Miyamoto & Kim, 1999). MIP1-α binds to G-protein-coupled receptors CCR1 and CCR5 leading to downstream processes important for many inflammatory conditions (Murdoch & Finn, 2000; Maurer & von Stebut, 2004). The majority of studies on microglial chemokine receptor expression and release focus on their role in neurodegenerative and inflammatory conditions (Hanisch, 2002). Due to low and undetectable levels of constitutive release, the roles of chemokines under physiological conditions are often neglected. Recent data suggest potential functions of chemokines in modulating normal brain activities in addition to their classical roles in inflammatory responses (Rostene *et al.* 2007).

There are a few recent studies which indicate a role of MIP1-α in brain development. During cerebellar development, physiologically activated microglia express MIP1-α during a defined time window between P7 and P14 (Cowell & Silverstein, 2003), thus at a developmental stage similar to that of our studies. Cowell and Silverstein also reported that MIP1-α-positive cells were frequently located near the processes and cell bodies of CCR1-immunoreactive cells during times of neuronal and glial maturation suggesting that MIP1-α plays a role in postnatal cerebellar development.

Using *in situ* hybridization, Tran *et al.* (2004) demonstrated the expression of CCR1 and CCR5, the receptors for MIP1-α, but also CCR2, CXCR3 and CXCR4 chemokine receptors by neural precursor cells in the dentate gyrus, subventricular zone of the lateral ventricle, and olfactory bulb. The effects of MIP1-α on astrocytes have also been described. MIP1-α and MCP-1 treatment promoted astrocyte migration *in vitro* possibly via novel astrocytic receptors (Heesen *et al.* 1996). Moreover, subnanomolar concentrations of MIP1-α could induce chemotactic responses in astrocytes *in vitro* (Tanabe *et al.* 1997). Oligodendrocytes are probably not affected since they lack the expression of MIP1-α receptors (Maysami *et al.* 2006). MIP1-α might even exert an autocrine effect on microglia since it affects migration and cytoskeleton reorganization *in vitro* (Cross & Woodroofe, 1999; Maciejewski-Lenoir *et al.* 1999). Microglial cells can acquire different states and the classical activated state is the full pro-inflammatory phenotype (Hanisch & Kettenmann, 2007). However, in our experimental model, we do not claim that the microglial cells are activated. Instead, we think that during development, the amoeboid phenotype may have its own characteristic state both distinct from the surveying (formerly resting) microglia and the fully blown pro-inflammatory phenotype. Taken together, our results suggest that GABA-triggered MIP1-α release has the potential to control some certain properties of microglia, astrocytes and precursor cells in the developing corpus callosum.

References

Aloisi F (2001). Immune function of microglia. *Glia* **36**, 165–179.

Ambrosini E & Aloisi F (2004). Chemokines and glial cells: a complex network in the central nervous system. *Neurochem Res* **29**, 1017–1038.

Bajetto A, Bonavia R, Barbero S & Schettini G (2002). Characterization of chemokines and their receptors in the central nervous system: physiopathological implications. *J Neurochem* **82**, 1311–1329.

Barres BA, Chun LL & Corey DP (1990). Ion channels in vertebrate glia. *Annu Rev Neurosci* **13**, 441–474.

Bekar LK, Jabs R & Walz W (1999). $GABA_A$ receptor agonists modulate K^+ currents in adult hippocampal glial cells in situ. *Glia* **26**, 129–138.

Ben-Ari Y, Gaiarsa JL, Tyzio R & Khazipov R (2007). GABA: a pioneer transmitter that excites immature neurons and generates primitive oscillations. *Physiol Rev* **87**, 1215–1284.

Berger T, Schnitzer J & Kettenmann H (1991). Developmental changes in the membrane current pattern, K^+ buffer capacity, and morphology of glial cells in the corpus callosum slice. *J Neurosci* **11**, 3008–3024.

Berger T, Walz W, Schnitzer J & Kettenmann H (1992). GABA- and glutamate-activated currents in glial cells of the mouse corpus callosum slice. *J Neurosci Res* **31**, 21–27.

Bergles DE, Roberts JD, Somogyi P & Jahr CE (2000). Glutamatergic synapses on oligodendrocyte precursor cells in the hippocampus. *Nature* **405**, 187–191.

Bormann J & Kettenmann H (1988). Patch-clamp study of γ-aminobutyric acid receptor Cl^- channels in cultured astrocytes. *Proc Natl Acad Sci U S A* **85**, 9336–9340.

Boucsein C, Kettenmann H & Nolte C (2000). Electrophysiological properties of microglial cells in normal and pathologic rat brain slices. *Eur J Neurosci* **12**, 2049–2058.

Brockhaus J, Ilschner S, Banati RB & Kettenmann H (1993). Membrane properties of ameboid microglial cells in the corpus callosum slice from early postnatal mice. *J Neurosci* **13**, 4412–4421.

Brockhaus J, Möller T & Kettenmann H (1996). Phagocytozing ameboid microglial cells studied in a mouse corpus callosum slice preparation. *Glia* **16**, 81–90.

Cowell RM & Silverstein FS (2003). Developmental changes in the expression of chemokine receptor CCR1 in the rat cerebellum. *J Comp Neurol* **457**, 7–23.

Cross AK & Woodroofe MN (1999). Chemokines induce migration and changes in actin polymerization in adult rat brain microglia and a human fetal microglial cell line in vitro. *J Neurosci Res* **55**, 17–23.

Cuadros MA & Navascues J (2001). Early origin and colonization of the developing central nervous system by microglial precursors. *Prog Brain Res* **132**, 51–59.

del Rio-Hortega P (1932). In *Cytology and Cellular Pathology of the Nervous System*, ed. Penfield W, pp. 481–534. Hoeber, New York.

Färber K, Pannasch U, Kettenmann H (2005). Dopamine and noradrenaline control distinct functions in rodent microglial cells. *Mol Cell Neurosci* **29**, 128–138.

Ferrer I, Bernet E, Soriano E, del Rio T & Fonseca M (1990). Naturally occurring cell death in the cerebral cortex of the rat and removal of dead cells by transitory phagocytes. *Neuroscience* **39**, 451–458.

Franchini L, Levi G & Visentin S (2004). Inwardly rectifying K^+ channels influence Ca^{2+} entry due to nucleotide receptor activation in microglia. *Cell Calcium* **35**, 449–459.

Gao XB & Van Den Pol AN (2000). GABA release from mouse axonal growth cones. *J Physiol* **523**, 629–637.

Haas S, Brockhaus J, Verkhratsky A & Kettenmann H (1996). ATP-induced membrane currents in ameboid microglia acutely isolated from mouse brain slices. *Neuroscience* **75**, 257–261.

Hamill OP, Marty A, Neher E, Sakmann B & Sigworth FJ (1981). Improved patch-clamp techniques for high-resolution current recording from cells and cell-free membrane patches. *Pflugers Arch* **391**, 85–100.

Hanisch UK & Kettenmann H (2007). Microglia: active sensor and versatile effector cells in the normal and pathologic brain. *Nat Neurosci* **10**, 1387–1394.

Hanisch UK (2002). Microglia as a source and target of cytokines. *Glia* **40**, 140–155.

Heesen M, Tanabe S, Berman MA, Yoshizawa I, Luo Y, Kim RJ, Post TW, Gerard C & Dorf ME (1996). Mouse astrocytes respond to the chemokines MCP-1 and KC, but reverse transcriptase-polymerase chain reaction does not detect mRNA for the KC or new MCP-1 receptor. *J Neurosci Res* **45**, 382–391.

Heinemann U & Arens J (1992). Production and calibration of ion-sensitive microelectrodes. In *Practical Electrophysiological Methods*, ed. Kettenmann H & Grantyn R, pp. 206–212. Wiley-Liss, New York.

Hirasawa T, Ohsawa K, Imai Y, Ondo Y, Akazawa C, Uchino S & Kohsaka S (2005). Visualization of microglia in living tissues using Iba1-EGFP transgenic mice. *J Neurosci Res* **81**, 357–362.

Hoppe D & Kettenmann H (1989). GABA triggers a Cl^- efflux from cultured mouse oligodendrocytes. *Neurosci Lett* **97**, 334–339.

Kaila K, Panula P, Karhunen T & Heinonen E (1991). Fall in intracellular pH mediated by GABAA receptors in cultured rat astrocytes. *Neurosci Lett* **126**, 9–12.

Kann O, Kovacs R & Heinemann U (2003). Metabotropic receptor-mediated Ca^{2+} signaling elevates mitochondrial Ca^{2+} and stimulates oxidative metabolism in hippocampal slice cultures. *J Neurophysiol* **90**, 613–621.

Káradóttir R, Hamilton NB, Bakiri Y & Attwell D (2008). Spiking and nonspiking classes of oligodendrocyte precursor glia in CNS white matter. *Nat Neurosci* **11**, 450–456. Erratum in: *Nat Neurosci* (2008) **11**, 851.

Kettenmann H, Backus KH & Schachner M (1987). γ-Aminobutyric acid opens Cl^- channels in cultured astrocytes. *Brain Res* **404**, 1–9.

Kettenmann H, Hoppe D, Gottmann K, Banati R & Kreutzberg G (1990). Cultured microglial cells have a distinct pattern of membrane channels different from peritoneal macrophages. *J Neurosci Res* **26**, 278–287.

Kresse W, Sekler I, Hoffmann A, Peters O, Nolte C, Moran A & Kettenmann H (2005). Zinc ions are endogenous modulators of neurotransmitter-stimulated capacitative Ca^{2+} entry in both cultured and *in situ* mouse astrocytes. *Eur J Neurosci* **21**, 1626–1634.

Kirchhoff F & Kettenmann H (1992). GABA triggers a $[Ca^{2+}]_i$ increase in murine precursor cells of the oligodendrocyte lineage. *Eur J Neurosci* **4**, 1049–1058.

Kuhn SA, van Landeghem FK, Zacharias R, Farber K, Rappert A, Pavlovic S, Hoffmann A, Nolte C & Kettenmann H (2004). Microglia express $GABA_B$ receptors to modulate interleukin release. *Mol Cell Neurosci* **25**, 312–322.

Kuner T & Augustine GJ (2000). A genetically encoded ratiometric indicator for chloride: capturing chloride transients in cultured hippocampal neurons. *Neuron* **27**, 447–459.

Labrakakis C, Müller T, Schmidt K & Kettenmann H (1997). $GABA_A$ receptor activation triggers a Cl^- conductance increase and a K^+ channel blockade in cerebellar granule cells. *Neuroscience* **79**, 177–189.

Leinekugel X, Tseeb V, Ben-Ari Y & Bregestovski P (1995). Synaptic $GABA_A$ activation induces Ca^{2+} rise in pyramidal cells and interneurons from rat neonatal hippocampal slices. *J Physiol* **487**, 319–329.

Lin SC & Bergles DE (2002). Physiological characteristics of NG2-expressing glial cells. *J Neurocytol* **31**, 537–549.

Lin SC, Huck JH, Roberts JD, Macklin WB, Somogyi P & Bergles DE (2005). Climbing fiber innervation of NG2-expressing glia in the mammalian cerebellum. *Neuron* **46**, 773–785.

Maciejewski-Lenoir D, Chen S, Feng L, Maki R & Bacon KB (1999). Characterization of fractalkine in rat brain cells: migratory and activation signals for CX3CR-1-expressing microglia. *J Immunol* **163**, 1628–1635.

McManus CM, Brosnan CF & Berman JW (1998). Cytokine induction of MIP-1α and MIP-1β in human fetal microglia. *J Immunol* **160**, 1449–1455.

Marandi N, Konnerth A & Garaschuk O (2002). Two-photon chloride imaging in neurons of brain slices. *Pflugers Arch* **445**, 357–365.

Markovic DS, Glass R, Synowitz M, Rooijen N & Kettenmann H (2005). Microglia stimulate the invasiveness of glioma cells by increasing the activity of metalloprotease-2. *J Neuropathol Exp Neurol* **64**, 754–762.

Maurer M & von Stebut E (2004). Macrophage inflammatory protein-1. *Int J Biochem Cell Biol* **36**, 1882–1886.

Maysami S, Nguyen D, Zobel F, Heine S, Hopfner M & Stangel M (2006). Oligodendrocyte precursor cells express a functional chemokine receptor CCR3: implications for myelination. *J Neuroimmunol* **178**, 17–23.

Miyamoto Y & Kim SU (1999). Cytokine-induced production of macrophage inflammatory protein-1α (MIP-1α) in cultured human astrocytes. *J Neurosci Res* **55**, 245–251.

Müller T, Fritschy JM, Grosche J, Pratt GD, Möhler H & Kettenmann H (1994). Developmental regulation of voltage-gated K^+ channel and $GABA_A$ receptor expression in Bergmann glial cells. *J Neurosci* **14**, 2503–2514.

Müller T, Möller T, Berger T, Schnitzer J & Kettenmann H (1992). Calcium entry through kainate receptors and resulting potassium-channel blockade in Bergmann glial cells. *Science* **256**, 1563–1566.

Murdoch C & Finn A (2000). Chemokine receptors and their role in inflammation and infectious diseases. *Blood* **95**, 3032–3043.

Nolte C, Matyash M, Pivneva T, Schipke CG, Ohlemeyer C, Hanisch UK, Kirchhoff F & Kettenmann H (2001). GFAP promoter-controlled EGFP-expressing transgenic mice: a tool to visualize astrocytes and astrogliosis in living brain tissue. *Glia* **33**, 72–86.

Nolte C, Möller T, Walter T & Kettenmann H (1996). Complement 5a controls motility of murine microglial cells *in vitro* via activation of an inhibitory G-protein and the rearrangement of the actin cytoskeleton. *Neuroscience* **73**, 1091–1107.

Owens DF & Kriegstein AR (2002). Is there more to GABA than synaptic inhibition? *Nat Rev Neurosci* **3**, 715–727.

Pastor A, Chvatal A, Sykova E & Kettenmann H (1995). Glycine- and GABA-activated currents in identified glial cells of the developing rat spinal cord slice. *Eur J Neurosci* **7**, 1188–1198.

Perry VH, Hume DA & Gordon S (1985). Immunohistochemical localization of macrophages and microglia in the adult and developing mouse brain. *Neuroscience* **15**, 313–326.

Pocock JM & Kettenmann H (2007). Neurotransmitter receptors on microglia. *Trends Neurosci* **30**, 527–535.

Prinz M, Kann O, Draheim HJ, Schumann RR, Kettenmann H, Weber JR & Hanisch UK (1999). Microglial activation by components of gram-positive and -negative bacteria: distinct and common routes to the induction of ion channels and cytokines. *J Neuropathol Exp Neurol* **58**, 1078–1089.

Rostene W, Kitabgi P & Parsadaniantz SM (2007). Chemokines: a new class of neuromodulator? *Nat Rev Neurosci* **8**, 895–903.

Sakmann B & Trube G (1984). Conductance properties of single inwardly rectifying potassium channels in ventricular cells from guinea-pig heart. *J Physiol* **347**, 641–657.

Schipke CG, Ohlemeyer C, Matyash M, Nolte C, Kettenmann H & Kirchhoff F (2001). Astrocytes of the mouse neocortex express functional *N*-methyl-D-aspartate receptors. *FASEB J* **15**, 1270–1272.

Steinhäuser C, Berger T, Frotscher M & Kettenmann H (1992). Heterogeneity in the membrane current pattern of identified glial cells in the hippocampal slice. *Eur J Neurosci* **4**, 472–484.

Steinhäuser C, Jabs R & Kettenmann H (1994). Properties of GABA and glutamate responses in identified glial cells of the mouse hippocampal slice. *Hippocampus* **4**, 19–35.

Tanabe S, Heesen M, Berman MA, Fischer MB, Yoshizawa I, Luo Y & Dorf ME (1997). Murine astrocytes express a functional chemokine receptor. *J Neurosci* **17**, 6522–6528.

Tran PB, Ren D, Veldhouse TJ & Miller RJ (2004). Chemokine receptors are expressed widely by embryonic and adult neural progenitor cells. *J Neurosci Res* **76**, 20–34.

Van Rooijen N & Sanders A (1994). Liposome mediated depletion of macrophages: mechanism of action, preparation of liposomes and applications. *J Immunol Methods* **174**, 83–93.

von Blankenfeld G & Kettenmann H (1991). Glutamate and GABA receptors in vertebrate glial cells. *Mol Neurobiol* **5**, 31–43.

Von Blankenfeld G, Trotter J & Kettenmann H (1991). Expression and developmental regulation of a $GABA_A$ receptor in cultured murine cells of the oligodendrocyte lineage. *Eur J Neurosci* **3**, 310–316.

Ziskin JL, Nishiyama A, Rubio M, Fukaya M & Bergles DE (2007). Vesicular release of glutamate from unmyelinated axons in white matter. *Nat Neurosci* **10**, 321–330.

Acknowledgements

We thank Irene Haupt for excellent technical assistance. This research was supported by Deutsche Forschungsgemeinschaft and BMBF.

Supplemental material

Online supplemental material for this paper can be accessed at: http://jp.physoc.org/cgi/content/full/jphysiol.2008.163923/DC1